Improving the Estimation of Relative Earthquake Locations using Surface Waves with Source Corrections

Michael Howe & Göran Ekström

Lamont-Doherty Earth Observatory, Columbia University

PI: Göran Ekström , ekstrom@ldeo.columbia.edu (howe@ldeo.columbia.edu)

Consortium for Verification Technology (CVT)

Lamont-Doherty Earth Observatory
Columbia University | Earth Institute

Introduction

Surface waves are both the largest and the slowest-propagating signals recorded on a seismogram. Arrival-time differences for different earthquakes with relatively small inter-event distances give information about the relative location of those earthquakes. A demonstration of the effectiveness of surface-wave relocation can be seen in **Figure 1**. The localization of earthquakes onto linear segments is consistent with the pattern of seismicity anticipated from plate tectonics. These earthquakes, near the Balleny Islands in the southern Pacific Ocean, are well suited to this method since they are predominantly strike-slip and normal-faulting earthquakes. The type of earthquake source is very important to this type of relocation technique, since some earthquake geometries generate phase shifts in the recorded seismograms that can mimic a location shift. The corrections required to account for arbitrary earthquakes geometries in the application of the surface-wave relocation is the focus of the remainder of this poster.

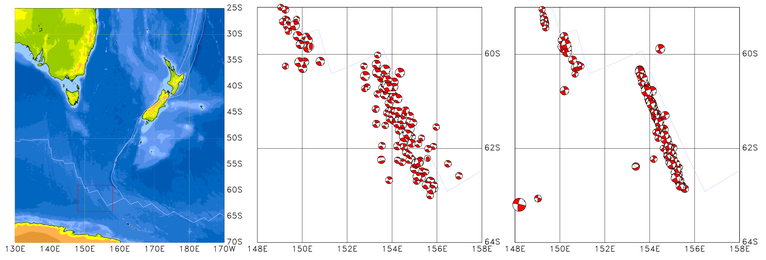

Figure 1: *(Left) Ridge-transform system near the Balleny Islands south of New Zealand. Initial (Middle) and Relocated (Right) epicenters in a ridge-transform tectonic setting near the Balleny Islands. Significant location improvement when comparing before (top) and after (bottom) surface wave relocations. The gray lines are mapped plate boundaries (Bird, 2003).*

Theory

We measure time lag of the cross-correlation between the recorded waveforms of two events within a prescribed inter-event distance. If the effect of the receiver is removed, each waveform can be expressed as a convolution of the effects of the path of propagation (Green Function) and the effects of the source. In the frequency domain, this is a product of those two terms, as shown in **Equations 1 and 2**. The cross-correlation of these two waveforms is (again in the frequency domain) the complex conjugate of waveform A multiplied by waveform B, as in **Equation 3**.

$$u^A(\omega) = G^A(\omega)S^A(\omega) \quad (1)$$

$$u^B(\omega) = G^B(\omega)S^B(\omega) \quad (2)$$

$$S(\omega) = R(\omega) + iJ(\omega) \quad (3)$$

$$\begin{aligned} C^{AB}(\omega) &= G^A G^{B*} S^{A*} S^B \\ &= G^A G^{B*} \cdot [R^A R^B - J^A J^B + \\ &\quad i(R^A J^B - J^A R^B)] \end{aligned} \quad (4)$$

The cross-correlation function in **Equation 4** includes a phase shift from the earthquake radiation patterns if the imaginary component (J) is non-zero. In order to remove this effect, we calculate the *R* and *J* for each earthquake, and then (as shown in **Equation 5**) divide the cross-correlation by the source effects of the two earthquakes. An example of what this effect looks like for Rayleigh waves of two example earthquakes is shown in Figure 2.

$$C^{AB}_{corr}(\omega) = \frac{C^{AB}(\omega)}{S^{A*}S^B} \quad (5)$$

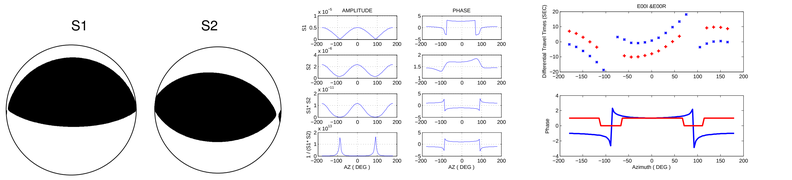

Figure 2: *(Left) Focal mechanisms of a shallow-dipping thrust earthquake and upper-plate thrust earthquake. (Middle) Amplitudes and Phases of the radiation patterns of the two earthquakes (top two rows) and the combined radiation pattern. (Right) Differential travel times without (blue) and with (red) source corrections in the top row. The red line in the bottom-right plot depicts which azimuths to omit and which to retain.*

Synthetic Data - Simulated Subduction Zone

We conducted a synthetic experiment, simulating a subduction zone, dipping from south to north, with 4 outer-rise normal-faulting events, 3 upper-plate thrust-faulting events and 12 interplate megathrust events. Figure 3 shows the true, initial and relocated epicenters for these 19 synthetic earthquakes.

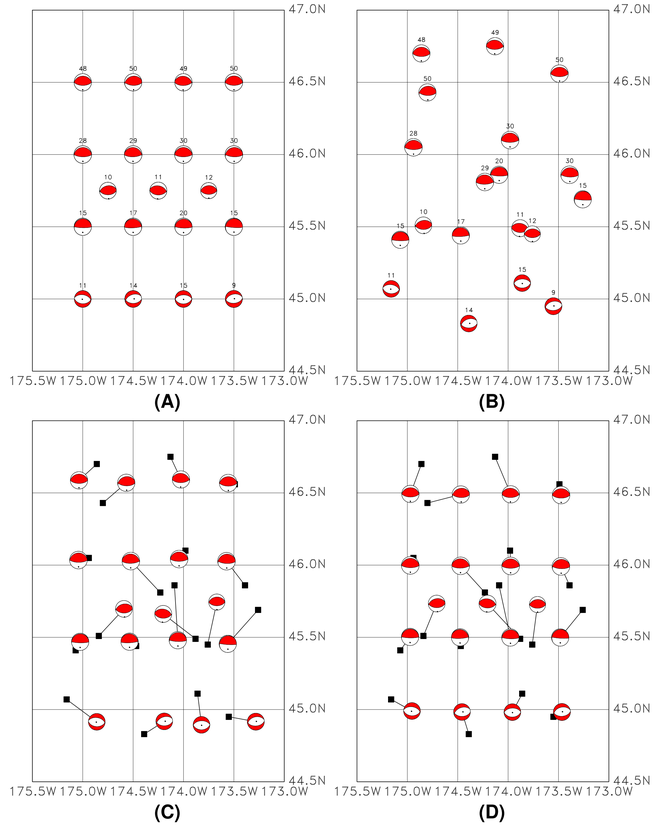

Figure 3: *(A) True locations of 19 earthquakes used in a synthetic experiment. (B) Initial locations assumed when making source corrections and relocation calculations. (C) Surface wave relocations without any source corrections. (D) Surface wave relocations with source corrections made for each event.*

Relocated epicenters that use source corrections are more accurate than epicenters relocated without using source corrections. Figure 4 shows the distribution of location errors for each relocation method, as well as an example of differential travel times without and with source corrections.

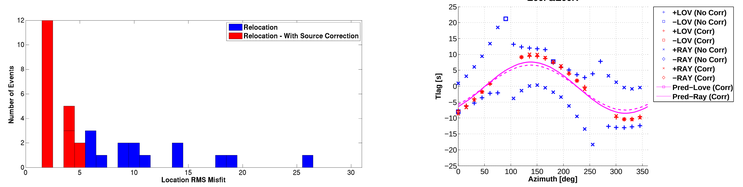

Figure 4: *(Left) Distribution of location error of the 19 synthetic events without (blue) and with (red) source corrections. (Right) Example of two inter-event pair cross-correlation measurements between the same two synthetic earthquakes analyzed in Figure 2.*

Real Data - Aleutian Island Arc

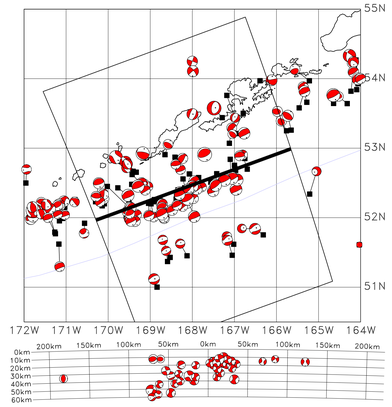

Figure 5: *(TOP) Relocated epicenters of real earthquakes in the Aleutian Island Arc using source corrections. (BOTTOM) Cross-section with a viewing direction to the northeast of the events with in the box.*

We applied our relocation procedure to real earthquakes in a subduction system in a segment of the Aleutian Island Arc. Figure 5 shows the initial and relocated epicenters for 126 earthquakes.

Since we do not know the true locations for these real earthquakes, we rely on an alternative metric to assess the location uncertainties. To do this, we relocate each earthquake using various subsamples of the data available. The diameter of the smallest circle that encloses all the subsampled locations we define as the empirical uncertainty of the new location. Using this empirical uncertainty to assess the quality of the relocated epicenters, we also decide which period bands to use for the inversion. Figure 6 shows the comparison of empirical uncertainties for relocations using a short period band (29–40 s), a long period band (46–64 s), and using both period bands together.

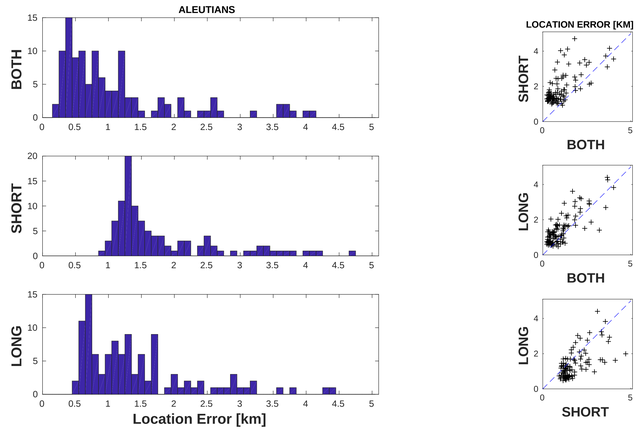

Figure 6: *(LEFT) Histograms of the empirical uncertainties of the relocations in the Aleutian Island Arc for each passband. (RIGHT) Comparison of the empirical uncertainties for each passband against each other.*

Forthcoming Research

Building upon this work, we will apply our relocation procedure to a large plate margin system. We will use parameters of quality control discovered in the development of the procedure to systematically relocate earthquakes within the region.

Acknowledgements

This work was funded in part by the Consortium for Verification Technology under the Department of Energy National Nuclear Security Administration award number DE-NA0002534 and the National Science Foundation under award EAR-1520657. The data used was obtained from the GSN through the USGS and IRIS.